Recovery of Xanthan Gum from Palm Oil-Based Fermentation Broth by Diafiltration with Flat Polysulfone Microfiltration (MF) Membrane

M. Sufian So'aib,[a,*] J. Krishnan,[a] and M. V. P. S. Veluri[b]

[a]Faculty of Chemical Engineering, Universiti Teknologi MARA (UiTM), 40000, Shah Alam, Selangor

[b]Faculty of Chemical Engineering, Manipal International University, 71800, Nilai, Negeri Sembilan Darul Khusus, Malaysia

doi: 10.15255/CABEQ.2014.1926

Original scientific paper
Received: January 30, 2014
Accepted: September 3, 2014

Xanthan gum recovery from palm oil-based broth by diafiltration was carried out using flat microfiltration (MF) membrane. Optimization of process parameters such as transmembrane pressure (TMP), crossflow velocity (CFV), ionic strength (IS) and diafiltration factor (DF) was performed by Taguchi method using signal-to-noise (S/N) ratio of larger-the-better criterion yielding the following optimum conditions: level 1, level 2, level 3, and level 2, respectively, corresponding to Xanthan recovery of 68 %. Analysis of variance (ANOVA) showed the significance of TMP on providing a driving force for Xanthan's transmembrane transport (XTT), whereas little effect of DF indicated the evidence of sieving action by cake layer on XTT, which was also responsible for complete rejection of oil indicated by the absence of fatty acid component in permeate upon GC-MS analysis. On the contrary, better XTT was observed during MF operation on zero-oil broth due to absence of oily cake layer rendering CFV more effective.

Key words:

xanthan recovery, xanthan's transmembrane transport, Taguchi method

Introduction

Xanthan gum is a pseudoplastic biopolymer used as stabilizing agent in food, beverages, pharmaceutical, and cosmetic products, as well as drilling fluid in oil recovery.[1] A major hurdle for optimum Xanthan yield is poor oxygen transfer due to viscosity increase over fermentation hours that restrict crucial oxygen transfer for cell's metabolism. The use of bubble column and centrifugal fibrous-bed fermenter improved oxygen transfer slightly, resulting in Xanthan yield of 25–35 g L^{-1} compared to 22 g L^{-1} of conventional fermenter. Others resorted to biphasic water-in-oil (W/O) broth that successfully reduced Xanthan viscosity by dispersing Xanthan molecules within aqueous phase, resulting in Xanthan yield up to 65–75 g L^{-1}.[2]

The prospect optimum, industrial scale of Xanthan production utilizing W/O broth requires a feasible separation to replace the costly conventional separation and purification method that is attributed to energy-intensive centrifugation for cell separation from the whole broth, and massive amount of alcohol to separate Xanthan from liquid broth, i.e. at 1:3 of liquid: alcohol ratio.[2,3]

The potential substitute for conventional method of Xanthan recovery is membrane filtration. Previously, ultrafiltration (UF) was used to dewater and concentrate Xanthan solution,[4] whereas electrofiltration was used to concentrate Xanthan by electrophoretic effect.[5] In fact, membrane filtration is already common in the recovery and purification of other bioproducts, such as surfactin (biosurfactant),[6] fumaric acid,[7] alginate,[8] penicillin G[9] and enzymes.[10] More extensive application of membrane was shown during purification of protein implementing microfiltration (MF) for cell separation from whole broth followed by-product's concentration by UF or nanofiltration (NF).[11] To the best of our knowledge, similar strategy was never adopted for Xanthan recovery, except in our recent work employing hollow fibre MF membrane that results in 64 % recovery.[12]

This work demonstrated the feasibility of MF for Xanthan recovery from palm oil based (W/O) fermentation broth by optimizing the membrane filtration parameters using Taguchi method; transmembrane pressure (TMP), crossflow velocity (CFV) and ionic strength (IS) with diafiltration factor (DF) as additional parameter.

* Corresponding author: e-mail: sufian5129@salam.uitm.edu.my, tel.: +603 55438418, fax: +603 55436300

Materials and methods

Xanthan gum preparation

Xanthan was produced via fermentation in W/O broth using the method described in detail elsewhere.[12] The fermentation was carried out in 50 % (v/v) oil fraction in a 7 L bioreactor (INFORS HT) with 4.5 L working volume.

Membrane and experimental setup

Membrane filtration unit used was a crossflow type manufactured by PALL Corp., purchased from PALL (M) Distributor, and equipped with flat membrane channel, digital flow meter, manual valves, and built-in monitoring panel. Pressure was varied by adjusting manual valves, while the corresponding TMP was measured by digital monitor. The membrane was purchased from PALL (Centramate model). An additional tank and peristaltic pump were added to the equipment to supply diafiltrate buffer solution (distilled water) during diafiltration. The schematic diagram of crossflow filtration unit is shown in Fig. 1. The whole broth was diluted 10 times before used as filtration feed. Membrane characteristics are described in Table 1.

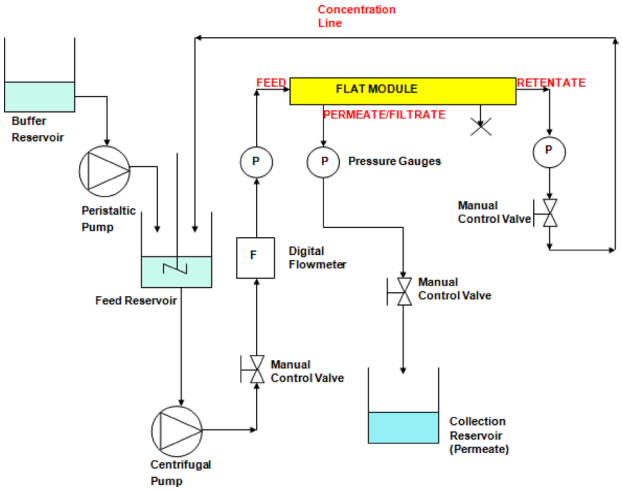

Fig. 1 – *Schematic diagram of laboratory scale crossflow filtration unit*

Table 1 – *Characteristics of the membrane used in the experiment*

	MF
Material	Polysulfone
Tolerable pH range	4–11
Maximum pressure (bar)	6.8
Effective surface area (m^2)	0.093
Pore size	0.2 μm
Maximum operating temperature (°C)	50

Fresh membrane was rinsed thoroughly by NaOH solution (0.2 mol L^{-1}) for 1 h to remove storage agent, followed by distilled water for another 1 h. The initial pure water flux J_w, (m^3 m^{-2} s^{-1}) was determined from Darcy's equation:

$$J_w = \frac{1}{A}\frac{\mathrm{d}V}{\mathrm{d}t} \tag{1}$$

where A is effective membrane area (m^2), V is permeate volume (m^3) and t is filtration time (s).

At the end of experiment, membrane module was cleaned by sodium dodecyl sufonate (0.1 %) for 1 h and soaked overnight in NaOH solution (0.1 mol L^{-1}). Before starting the next run, membrane module was rinsed with NaOH solution (0.2 mol L^{-1}) for 1 h, followed by citric acid (1 %) for 1 h, and finally rinsed with distilled water. Using the above Darcy's equation, post-cleaning water flux J_s (m^3 m^{-2} s^{-1}) was determined to measure cleaning efficiency/membrane recovery (FR).

$$FR = \frac{J_s}{J_w}\cdot 100\,\% \tag{2}$$

During diafiltration mode, buffer solution (distilled water) was pumped into feed reservoir by a peristaltic pump at flow rate equal to permeate flow rate to maintain constant volume as shown in Fig. 1. Diafiltration mode consists of three stages, namely pre-concentration, diafiltration, and post-concentration, defined as follows:

1) Pre-concentration, $a = \frac{V_d}{V_0}$ (3)

2) Diafiltration factor, $DF = \frac{V_w}{V_d}$ (4)

3) Post-concentration, $c = \frac{V_e}{V_d}$ (5)

where V_0 is initial feed volume, V_d is constant volume of tank during diafiltration mode, V_w is the volume of buffer (pure water) added to feed tank, V_e is final feed volume. a and c were kept constant at 2/3 and 1/3, respectively. Diafiltration factor (DF) was varied for optimisation. Diafiltration process is described in Fig. 2.

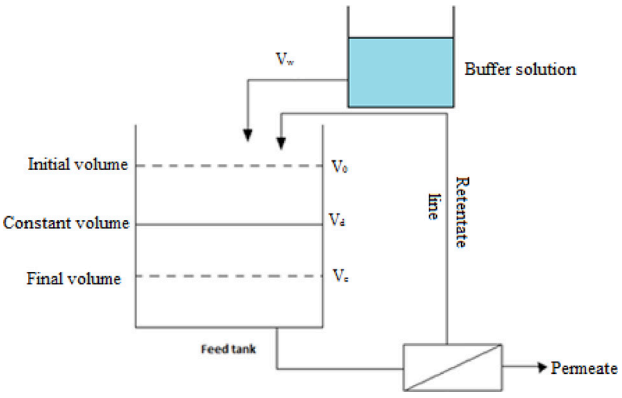

Fig. 2 – *Diafiltration process layout*

Determination of Xanthan concentration

Xanthan concentration was determined by dry weight method. First, cell was separated by centrifugation at 12 000 rpm for 15 minutes. The supernatant was precipitated by isopropanol (IPA) at volume ratio IPA: supernatant of 3:1. The precipitate was dried overnight in an oven at temperature 60 °C and weighed. The Xanthan recovery (R/%) was calculated as follow:

$$R/\% = \frac{C_P}{C_F} \cdot 100\,\% \tag{6}$$

where C_P is Xanthan concentration in permeate, C_F is Xanthan concentration in initial feed.

Determination of oil presence

The permeate quality in terms of oil presence was analysed by gas chromatography (GC) equipped with a mass spectrometer (MS) detector. A fused silica capillary column of 30 m × 0.32 mm ID, film thickness 0.25 μm was installed. The oven temperature was programmed as follow: 80 °C hold for 2 minutes at 20 °C min^{-1} until 125 °C (hold for 1 minute), then raised to 220 °C (hold for 3 minutes) at 3 °C min^{-1}. The injector and detector were operated at 240 °C. Nitrogen was used as carrier gas at flow rate 1 mL min^{-1} and a split ratio 1:10 was applied. Pure palm oil was used as standard. Each pure, initial feed and permeate sample was mixed with hexane in 2 mL sample cells to dissolve the palm oil residue.

Scanning electron microscopy (SEM)

The change in membrane's morphology due to fouling was examined by mini-scanning electron microscopy (SEM)-FEI Phenom at accelerating voltage 5.0 kV. The sample was dried and coated with a thin layer of gold prior to analysis. Scanning was made at 2000 and 6200 times magnification. This procedure was conducted on clean, fouled, and post-cleaning membrane.

Atomic force microscopy (AFM)

The image of membrane's top surface was obtained by using XE-100 Park AFM system (South Korea) operating in contact mode from a scanning area of 10 μm × 10 μm. Membrane was dried at ambient prior to analysis. Membrane's surface characterisation was made in terms of mean roughness (R_a), root mean square roughness (R_{rms}) and mean difference of height between five highest points and five lowest points (R_z). This procedure was conducted on clean, fouled, and post-cleaning membrane to observe the impact of fouling on membrane's morphology.

Design of experiment (DOE) method and analysis of variance (ANOVA)

Operating conditions of membrane filtration are described in Table 2. The study on the effect of factors and process optimisation were carried out by Taguchi method. All factors were varied simultaneously using Taguchi's orthogonal array (OA) and the effect of interacting factors can be determined from a specific column of OA according to its linear graph. This greatly reduced the number of experimental trials as opposed to trial and error approach where above experimental plan requires $3^4 = 81$ to investigate all possible combinations. The selection of appropriate OA must consider the degree of freedom (DOF) of the experimental plan. The above experimental plan which involves four factors at three levels each has eight DOF, i.e. $n(k–1)$ where n is the number of factor, and k is the number of levels. Therefore, the selected OA should have at least eight DOF or more. L_9 (3^4) OA met this criterion where it has four columns, each column can accommodate a factor at three levels, hence its total DOF is 8. The DOE of L_9 (3^4) OA is shown in Table 3. Xanthan recovery was chosen as the response. Experimental trials were randomised to minimise noise effect.[13]

Table 2 – *Operating parameters and levels*

Factor	Level		
	1	2	3
A. TMP, Transmembrane pressure (bar)	1.0	1.5	2.0
B. CFV, Crossflow velocity (min^{-1})	1.0	1.5	2.0
C. IS, Ionic strength (M)	0.1	0.5	0.8
D. DF, Diafiltration factor	1.0	1.5	2.0

Table 3 – *DOE based on L_9 (3^4) Taguchi's orthogonal array*

Trial	Factors and Levels			
	A	B	C	D
1	1	1	1	1
2	1	2	2	2
3	1	3	3	3
4	2	1	2	3
5	2	2	3	1
6	2	3	1	2
7	3	1	3	2
8	3	2	1	3
9	3	3	2	1

Taguchi recommends a standard method for result analysis. A loss function was used to measure the deviation from desired value, which can be quantified by signal-to-noise (S/N) ratio. Since maximum Xanthan recovery is desirable, S/N ratio larger-the-better criterion was used;

$$S/N = -10\log\left(\frac{1}{n}\sum_{i=1}^{n}\frac{1}{y_i^2}\right) \quad (7)$$

where n is the number of repetition, y_i is the response's value at ith trial.

The average S/N of each level of factor was calculated, where the optimum condition was indicated by the highest average S/N. Since there was a possibility that the optimum condition was not performed by any trial condition of above L_9 (3^4) OA, the predicted optimum Xanthan recovery (Y_{opt}) was calculated based on optimum condition determined by S/N ratio using the following additivity equation:[14]

$$Y_{opt} = \bar{T} + (\bar{A}_i - \bar{T}) + (\bar{C}_j - \bar{T}) + (\bar{D}_j - \bar{T}) \quad (8)$$

where $\bar{T}$ is average of all performance results (recovery), $\bar{A}_i$, $\bar{C}_j$ and $\bar{D}_k$ are average response of the significant factors at their respective optimum level i, j, k, etc.

The predicted result should fall within an acceptable range of error, in this case 95 % confidence level was chosen. The confidence interval (CI) was calculated as follows:

$$CI = \pm\sqrt{(F(1,n_2)\cdot v_e / N_e} \quad (9)$$

where $F(1, n_2)$ = F value from the F Table at required confidence level at DOF 1 and error DOF n_2

v_e = variance of error term (from ANOVA)

N_e = Total number of results (or number of S/N ratios) / DOF of mean (=1, always) + DOF of all factors included in the estimate of mean

Results in terms of percentage were converted into omega (Ω) term before eqs. 7–8 were applied. This was to avoid unrealistic additivity value in case of poor additivity, e.g. percentage value is very close to 0 % or 100 %.[15]

$$\Omega = -10\log\left(\frac{1}{p} - 1\right) \quad (10)$$

where p is fractional value of percentage (e.g. p = 0.58 = 58 %).

Results in terms of S/N ratio were converted back to original term at the end of analysis.

Results and discussion

Taguchi result

The results of Taguchi's L_9 (3^4) OA experimental design is shown in Table 4. The average S/N ratio of each level of main factors is shown in Fig. 3 which

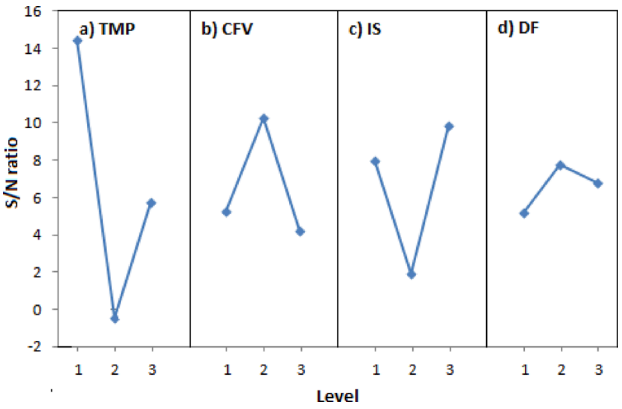

Fig. 3 – *S/N ratio plot of main effect a) Transmembrane pressure b) Crossflow velocity c) Ionic strength d) Diafiltration factor*

Table 4 – *Result of L_9 (3^4) Taguchi's orthogonal array*

Trial	Factor				Recovery (%)			Ω (db)		SN_L
	A	B	C	D	1	2	Average	1	2	
1	1	1	1	1	2	32	17	–16.9	–3.27	13.15
2	1	2	2	2	19	25	22	–6.3	–4.77	14.61
3	1	3	3	3	24	14	19	–5.01	–7.88	15.53
4	2	1	2	3	48	68	57	–0.35	3.274	–6.22
5	2	2	3	1	42	67	54	–1.4	3.076	5.12
6	2	3	1	2	31	54	42	–3.47	0.696	–0.30
7	3	1	3	2	23	38	31	–5.25	–2.13	8.90
8	3	2	1	3	35	85	60	–2.69	7.533	11.08
9	3	3	2	1	53	11	32	0.522	–9.08	–2.65

suggests that varying TMP caused a significant effect on the response, whereas a minimal effect was observed by varying DF. The optimum level of each factor is indicated by the highest peak of S/N plot.

Effect of TMP

TMP provides a driving force to facilitate XTT, which stood at the optimum level 1 in the range studied. Any membrane operation is susceptible to concentration polarisation and fouling, especially during operation above critical flux. This was the likely condition at the higher level of TMP due to increase in the rate of particle deposition on the membrane surface. If such phenomenon occurred, Xanthan solubility, which quickly reached the maximum within a gel layer boundary close to the membrane surface could create osmotic pressure and presented re-entraining force in the opposite direction to TMP's driving force, thus reduced effectiveness of TMP to drive XTT.[16] As observed in the earlier study on filtration of biopolymer, although a gel layer was initially reversible, higher TMP unfavourably pushed the molecules within close vicinity to one another, resulting in a more compact gel layer and reduced reverse mass transport, which later transformed into cake layer and internal fouling.[17] In the context of this study, cake layer and fouling acted as a sieving mechanism which prevented Xanthan's transmembrane transport.

Effect of CFV

Earlier study suggested that hydrodynamic shear reduces Xanthan's viscosity due to Xanthan's shear-thinning behavior,[4] thus minimising gel layer formation. Higher CFV, which was optimum at level 2, might have reflected this effect. However, the least Xanthan recovery at the highest CFV hinted significant physico-chemical interaction of Xanthan-membrane or among Xanthan-Xanthan which formed stable adsorptive layer and molecule's aggregation, respectively. Xanthan's adsorptive layer might have been more stable towards the end of the filtration process together with the increase in aggregate population, which hindered Xanthan's transmembrane transport. At this stage, higher CFV i.e. at level 3 undermined the driving force of TMP acting normal to the membrane surface, which was critical for Xanthan's transmembrane transport.

Effect of IS

Intramolecular interaction between Xanthan's functional groups via H-bond is a strong function of ionic strength. Hence, the purpose of salt addition was to create intramolecular shielding between Xanthan's functional group so that Xanthan's particles could be reduced to a smaller size of spherocolloidal shape to ease transmembrane transport, as well as screening membrane-Xanthan repulsion by modifying membrane's surface charge through cation binding on the membrane surface.[18,19] Since continuous addition of diafiltrate buffer caused depletion of salt concentration, higher salt concentration, i.e. at level 3, was necessary to bring a favourable effect of particle size decrease. In addition, higher cation concentration favourably led to in-pore accumulation of charge density to cause pore swelling due to repulsion between counterions to allow a greater degree of Xanthan permeation.

Effect of DF

The addition of diafiltrate buffer during diafiltration stage delayed the saturation of Xanthan at the membrane surface, as observed from the drop of Xanthan concentration at retentate side during diafiltration mode, shown in Fig. 4, thus slowing down the rate of concentration polarisation formation. Such effect contributed to the effectiveness of TMP to drive XTT, which was later proved by ANOVA. However, little effect of varying DF on Xanthan recovery suggests the existence of cake layer on the membrane surface at any point during MF operation, which sieved Xanthan.

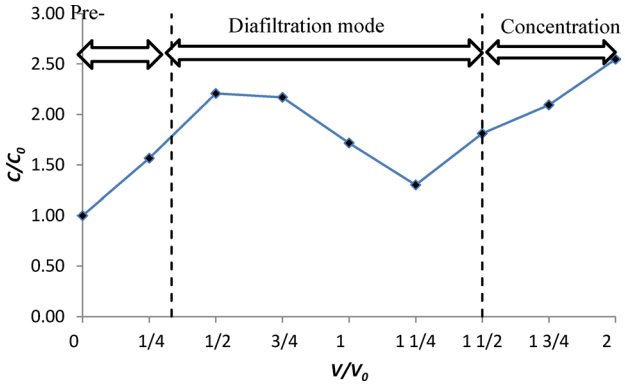

Fig. 4 – *Xanthan concentration (C) normalised to initial Xanthan concentration C_0 vs cumulative permeate volume*

ANOVA results

ANOVA was conducted to study the influence of each factor on average response and its statistical significance. *F*-test was carried out to study the significance of a factor with respect to error by calculating the ratio of factor's variance to error's variance. Higher F-ratio is desirable as it indicates the greater effect of a factor on the response compared to error. A factor which has two DOF becomes statistically significant with respect to error at 95 % confidence level if its *F*-ratio is at least equal to critical *F*-ratio. But converting response values of repeated trials into S/N ratio gave only a single response value in terms of S/N ratio for each trial condition; hence the DOF

of the entire experiment was eight, whereas DOF of error was zero. *F*-ratio cannot be determined in this case, unless one of the factors, which had the least effect on the response, indicated by its lowest sum of squares (SS), was chosen as an error term in a process known as pooling. Thus, DF which had the least (SS) was ignored. The pooled ANOVA result is shown in Table 5, showing the sum of squares (SS), DOF, variance (V), *F*-ratio, and percentage contribution (*P*/%) of each factor.

Table 5 – *Pooled ANOVA result for Xanthan recovery*

Factor	SS	DOF	V	*F*-ratio	F_{cr}	*P*/%
A	335.76	2	167.88	34.22	19	65.58
B	63.11	2	31.56	6.43	19	12.33
C	103.27	2	51.63	10.52	19	20.17
D	(9.81)	(2)		Pooled		
Error	9.81	2	4.91			1.92
Total	511.95	8				100

It is noteworthy that TMP was statistically significant due to its *F*-ratio greater than F_{cr}; in other words, Xanthan recovery was most affected by varying TMP, but a very little effect could be expected from varying DF. Based on percentage contribution, also illustrated by Fig. 5, factors can be ranked according to the degree of significance in the following order: TMP>IS>CFV>DF. The reliability of the entire experiment was based on low contribution of 1.92 % error, which is well below the maximum error limit of 50 %.

Confirmation experiment

In order to validate the prediction of optimum Xanthan recovery derived from the results of Taguchi's experimental design, confirmation experiment was carried out using optimum condition based on level's effect on average S/N ratio. The observed result and predicted result at 95 % confidence interval are shown in Table 6. The observed result fell within calculated 95 % confidence interval, hence the experimental results using Taguchi method were within ±5 % error.

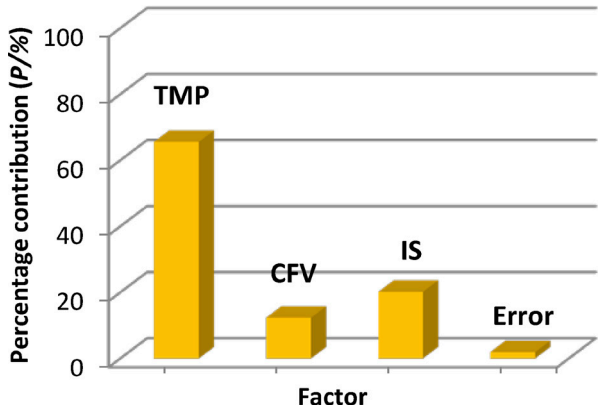

Fig. 5 – *Contribution of each factor to the response*

Table 6 – *Observed and predicted results at 95 % confidence level*

Factor	Optimum working condition	
	value	level
TMP, Transmembrane pressure (bar)	1.0	1
CFV, Crossflow velocity (min^{-1})	1.5	2
IS, Ionic strength (M)	0.8	3
V_w/V_d, Diafiltration ratio	1.5	2
Observed recovery (%)	68	
Predicted recovery (%)	93.7	
Predicted confidence interval (%)	65–99	

Effect of oil

The effect of oil on Xanthan recovery performance was investigated by conducting an experiment using zero-oil fermentation broth using the same operating conditions and DOE. All the relevant results are shown in Tables 7–8 and Fig. 6. Here, ANOVA result shows the significance of factors in the following order; CFV > IS > TMP > DF. The significance of CFV during zero-oil broth filtration indicates the greater effect of hydrodynamic shear to remove cake layer allowing greater passage of Xanthan. In contrast, the effect of hydrodynamic shear was severely undermined by oil cake layer stabilised by hydrophobic bond with membrane surface during previous filtration of oily broth. Again, there was little effect of varying the diafiltration factor (DF) which further proved that the particle size dependence of Xanthan's transmembrane transport was quickly halted by cake

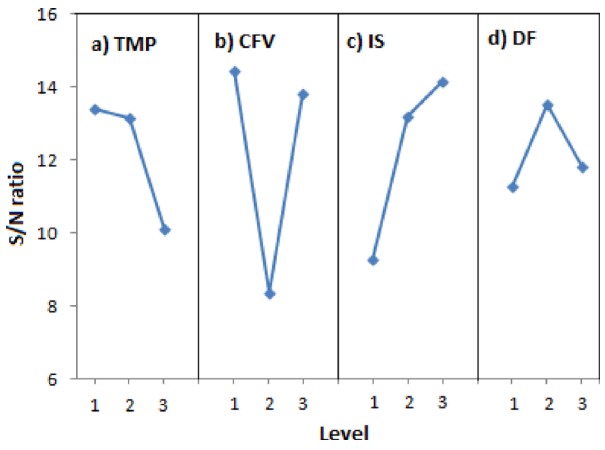

Fig. 6 – *S/N ratio plot of main effect a) Transmembrane pressure b) Crossflow velocity c) Ionic strength d) Diafiltration factor*

Table 7 – *L_9 (3^4) Taguchi's OA experimental result of zero oil broth filtration*

Trial	Factor				Recovery (%)	Ω (db)	SN_L
	A	B	C	D			
1	1	1	1	1	29	–3.89	11.80
2	1	2	2	2	29	–3.89	11.80
3	1	3	3	3	17.5	–6.73	16.57
4	2	1	2	3	81	6.30	15.98
5	2	2	3	1	32	–3.27	10.30
6	2	3	1	2	26	–4.54	13.15
7	3	1	3	2	20	–6.02	15.59
8	3	2	1	3	42	–1.40	2.93
9	3	3	2	1	29	–3.89	11.80

Table 8 – *ANOVA result for Xanthan recovery from aqueous broth filtration*

Factor	SS	DOF	V	*F*-ratio	*P*/%
A	20.02	2	10.01	2.496665	14.75
B	67.93	2	33.97	8.470907	50.05
C	39.76	2	19.88	4.95815	29.29
D	(8.02)	(2)		Pooled	
Error	8.02	2	4.01		5.91
Total	135.74				100

layer on membrane surface, despite low Xanthan concentration in bulk region which was due to continuous addition of diafiltrate buffer. The optimum level of each significant factor was no different from the previous oily broth filtration, except for CFV where the optimum stood at level 1. Xanthan recovery at optimum condition was obtained at 81 %.

Membrane characterization by atomic force microscopy (AFM)

A very distinct character can be observed in Fig. 7 between clean and fouled membrane in terms of the peak and valley appearance, i.e. the highest and the lowest point of the surface. Fouled membrane (Fig. 7 (b)) contained less valley appearance than the clean membrane (Fig. 7 (a)), which could be attributed to cake layer that filled the valley structure. The lowest R_a, R_{rms} and R_z values obtained for fouled membrane (Fig. 7 (b)) may have even resulted from layer of oil formed on membrane surface. This made the 3D image of fouled membrane to have less surface roughness as a result of reduced peak-to-valley distance.[20] 2D image of fouled membrane shows the original morphology was fully covered by foulant. The original morphology was restored partially after the cleaning process, as shown in Fig. 7 (c).

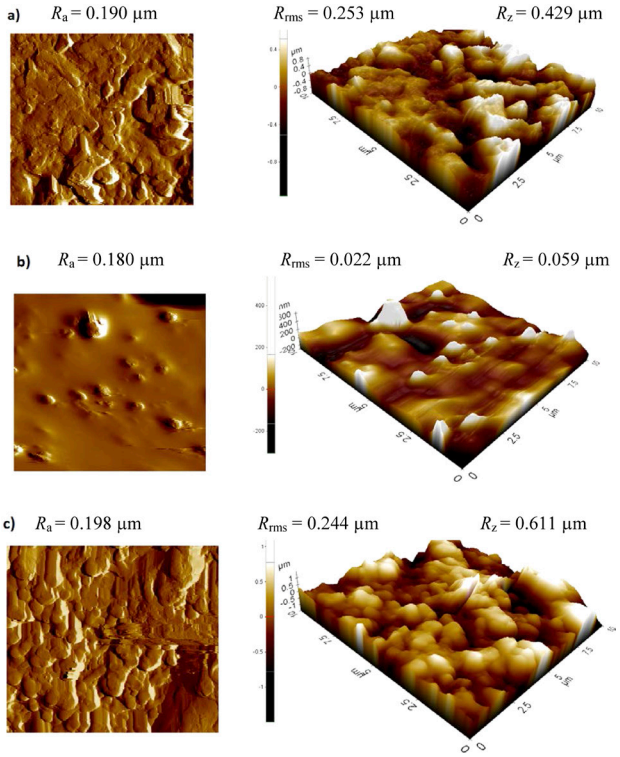

Fig. 7 – *AFM images of MF Flat membrane a) Clean/fresh membrane b) Fouled membrane c) Post-cleaning membrane*

Membrane characterization by scanning electron microscopy (SEM)

The morphology of clean and fouled membrane was also displayed by SEM images at 2000 and 6000 times magnifications, as shown in Fig. 8. Similar to the finding from AFM analysis, the number

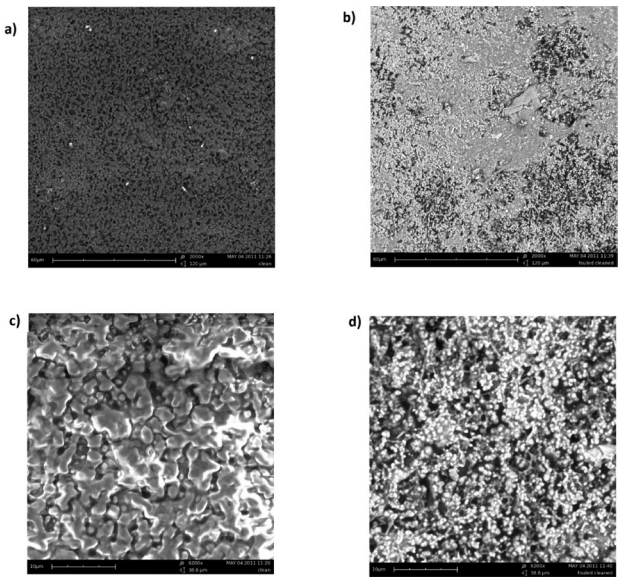

Fig. 8 – *SEM images of MF flat membrane a) Clean membrane (2000 times magnification) b) Fouled membrane (2000 times magnification) c) Clean membrane (6200 times magnification) d) Fouled membrane (6200 times magnification)*

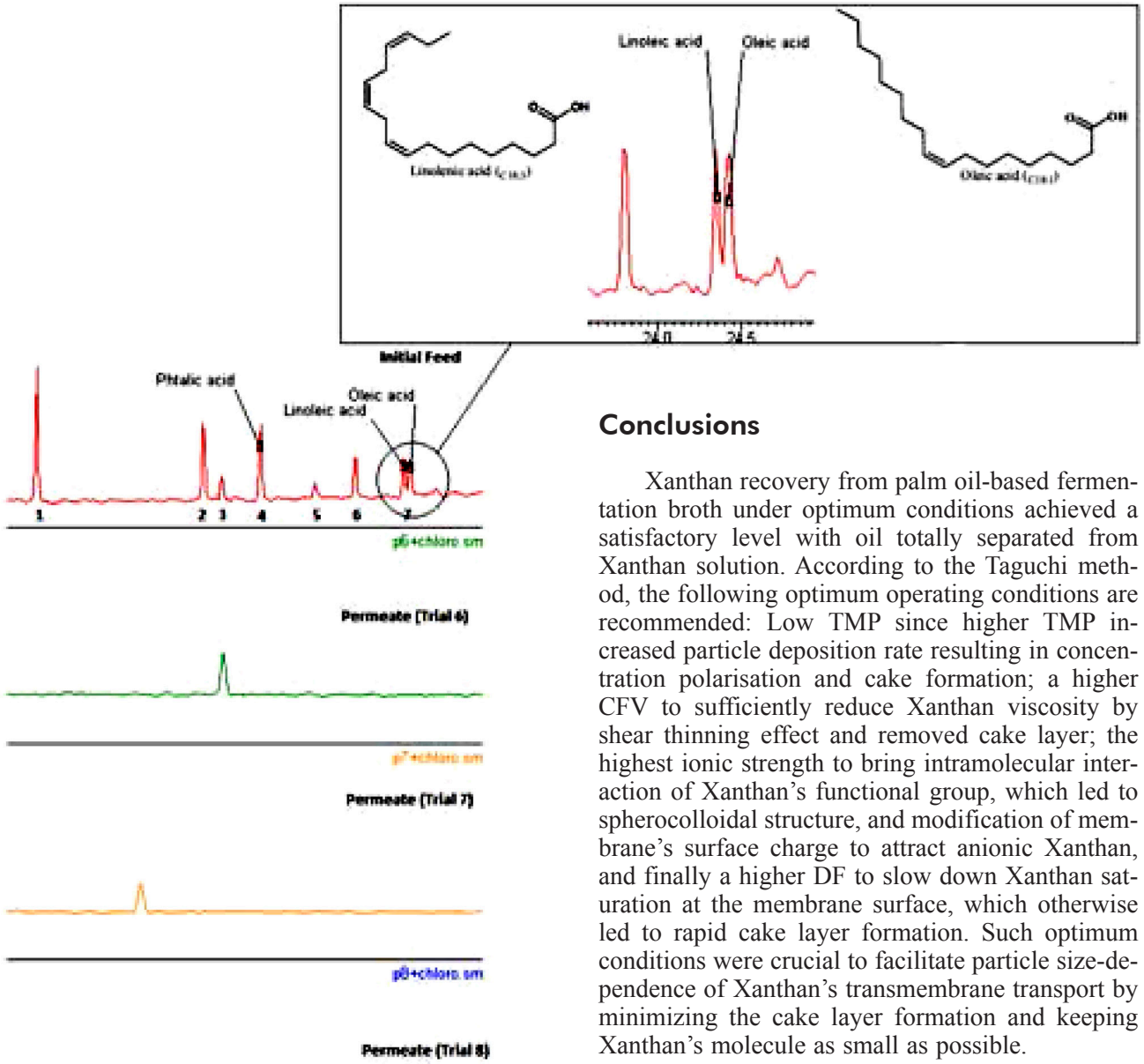

Fig. 9 – *Mass spectrometer peak of initial feed containing oil and permeate samples of several trial conditions*

of available pores originally observed on clean membrane was largely fouled by cake layer.

Oil residue detection by GC-MS

The presence of palm oil residue can be represented by its key fatty acid components; linoleic acid and oleic acid. From the results of GC-MS analysis, the peak appearance of permeate was compared with initial feed containing fatty acid residue. From Fig. 9, no fatty acid was detected in any of the permeate samples of all trial conditions, signifying complete oil retention by membrane surface, possibly as a result of coalescence by hydrodynamic forces. This also explained the single peak appearance of PSD analysis on permeate samples.

Conclusions

Xanthan recovery from palm oil-based fermentation broth under optimum conditions achieved a satisfactory level with oil totally separated from Xanthan solution. According to the Taguchi method, the following optimum operating conditions are recommended: Low TMP since higher TMP increased particle deposition rate resulting in concentration polarisation and cake formation; a higher CFV to sufficiently reduce Xanthan viscosity by shear thinning effect and removed cake layer; the highest ionic strength to bring intramolecular interaction of Xanthan's functional group, which led to spherocolloidal structure, and modification of membrane's surface charge to attract anionic Xanthan, and finally a higher DF to slow down Xanthan saturation at the membrane surface, which otherwise led to rapid cake layer formation. Such optimum conditions were crucial to facilitate particle size-dependence of Xanthan's transmembrane transport by minimizing the cake layer formation and keeping Xanthan's molecule as small as possible.

The MF on zero-oil broth revealed that the suspected oil cake layer stabilized by hydrophobic bond on the membrane surface which resisted higher Xanthan's transmembrane transport during MF on oily broth, although this layer favourably rejected oil, which may contaminate the permeate. The presence of oil at membrane upstream hampered the favourable effect of solution chemistry, which would otherwise create screening effect on intramolecular repulsion, to keep Xanthan as small sized spherocolloidal particles, and screening of Xanthan-membrane repulsive interaction through surface charge modification by cation binding.

ACKNOWLEDGEMENT

This work was financially supported by Ministry of Science, Technology and Innovation, (MOSTI) Malaysia through research grant No: 100-IRDC/SF 16/6/2(50/2007).

Abbreviations and symbols

AFM – atomic force microscopy
ANOVA – analysis of variance
CI – confidence interval
CFV – crossflow velocity, min^{-1}
DF – diafiltration factor
DOE – design of experiment
DOF – degree of freedom
FR – flux recovery, %
IPA – isopropyl alcohol
IS – ionic strength, M
MF – microfiltration
MS – mean of square
GC – gas chromatography
OA – orthogonal array
SEM – scanning electron microscopy
SS – sum of square
S/N – signal to noise
T – temperature, ºC
TMP – transmembrane pressure,bar
UF – ultrafiltration
W/O – water-in-oil
XTT – Xanthan transmembrane transport

Nomenclature

a – pre-concentration volume ratio
A – effective filtration area, m^2
c – post-concentration volume ratio
C_P – Xanthan concentration at permeate, g L^{-1}
C_F – solute concentration of initial feed, g L^{-1}
F_{cr} – critical F-ratio
J_0 – initial flux, $m^3\ m^{-2}\ s^{-1}$
J_w – pure water flux, $m^3\ m^{-2}\ s^{-1}$
J_s – post cleaning water flux, $m^3\ m^{-2}\ s^{-1}$
P – percent contribution, %
R – Xanthan recovery, %
R_a – mean roughness, µm
R_{rms} – root mean square roughness, µm
R_z – mean difference of height between five highest and five lowest points
t – filtration time, s
v/v – volume per volume, %
V_d – constant volume of tank during diafiltration mode, m^3
V_w – volume of buffer (pure water) added to feed tank, m^3
V_e – final feed tank volume, m^3
Y_{opt} – optimum Xanthan recovery

References

1. *Barbara, K.,* Polym. Degrad. Stab. **59** (1998) 81. http://dx.doi.org/10.1016/S0141–3910(97)00180–8
2. *Li, L., Dinga, L., Tua, Z., Wan, Y., Claussea, D., Lanoisellé, J.-L.,* J. Membr. Sci. **342** (2009) 70. http://dx.doi.org/10.1016/j.memsci.2009.06.023
3. *Lu-Kwang, J.*, Bioprocessing for Value-Added Products from Renewable Resources, Y. Shang-Tian, Elsevier, Amsterdam, 2007.
4. *Hofmann, R., Käppler, T., Posten, C.*, Sep. Purif. Technol. **51**(3) (2006) 303. http://dx.doi.org/10.1016/j.seppur.2006.01.015
5. *Isa, M. H. M., Frazier, R. A., Jauregi, P.*, Sep. Purif. Technol. **64**(2) (2008) 176–182. http://dx.doi.org/10.1016/j.seppur.2008.09.008
6. *Moresi, M., Ceccantoni, B., Lo Presti, S.*, J. Membr. Sci. **209**(2) (2002) 405. http://dx.doi.org/10.1016/S0376–7388(02)00330–7
7. *Moresi, M., Sebastiani, I., Wiley, D. E.*, J. Membr. Sci. **326**(2) (2009) 441. http://dx.doi.org/10.1016/j.memsci.2008.10.046
8. *Adikane, H. V., Singh, R. K., Nene, S. N.*, J. Membr. Sci. **162**(1–2) (1999) 119. http://dx.doi.org/10.1016/S0376–7388(99)00129–5
9. *Beier, S. P., Jonsson, G.,* Sep. Purif. Technol. **53**(1) (2007) 111. http://dx.doi.org/10.1016/j.seppur.2006.06.019
10. *Zhou, H., Ni, J., Huang, W., Zhang, J.,* Sep. Purif. Technol. **52**(1) (2006) 29. http://dx.doi.org/10.1016/j.seppur.2006.03.011
11. *Kuttuva, S. G., Restrepo, A. S., Ju, L. K.*, Appl. Microbiol. Biotechnol. **64** (2004) 340. http://dx.doi.org/10.1007/s00253–003–1461-x
12. *So'aib, M. S., Sabet, M., Krishnan, J., Veluri, M. V. P. S.,* Chem. Biochem. Eng. Q. **27**(2) (2013) 145.
13. *Safarzadeh, M. S., Moradkhani, D., Ilkhchi, M. O., Golshan, N. M.*, Sep. Purif. Technol. **58** (2008) 367. http://dx.doi.org/10.1016/j.seppur.2007.05.016
14. *Gönder, Z. B., Kaya, Y., Vergili, I., Barlas, H.*, Sep. Purif. Technol. **70** (2010) 265. http://dx.doi.org/10.1016/j.seppur.2009.10.001
15. *Ross, P. J.*, Taguchi Techniques for Quality Engineering, McGraw Hill, New York, 1996, pp 230–250.
16. *Moresi, M., Sebastiani*, *I.,* J. Membr. Sci. **322**(2) (2008) 349. http://dx.doi.org/10.1016/j.memsci.2008.05.066
17. *Van den Brink, P., Zwijnenburg, A., Smith, G., Temmink, H.,Van Loogrecht, M.*, J. Membr. Sci. **345**(1–2) (2009) 207. http://dx.doi.org/10.1016/j.memsci.2009.08.046
18. *Al-Amoudi, A., Lovitt, R. W.,* J. Membr. Sci. **303** (2007) 4. http://dx.doi.org/10.1016/j.memsci.2007.06.002
19. *Torrestiana-Sanchez, B., L. Balderas-Luna, De la Fuente, E. B., Lencki, R. W.*, J. Membr.Sci. **294** (2007) 84. http://dx.doi.org/10.1016/j.memsci.2007.02.014
20. *Nanda, D., Tung, K.-L., Li, Y.-L., Lin, N.-J., Chuang*, *C.-J.,* J. Membr. Sci., **349 (**2010) 411. http://dx.doi.org/10.1016/j.memsci.2009.12.004